Constant-Pressure Molecular Dynamics Techniques Applied to Complex Molecular Systems and Solvated Proteins

Emanuele Paci and Massimo Marchi*

Section de Biophysique des Protéines et Membranes, DBCM, DSV, CEA, Centre d'Etudes, Saclay, 91191 Gif-sur-Yvette Cedex, France

Received: October 6, 1995; In Final Form: November 28, 1995[⊗]

To assess the feasibility of high-pressure simulation of biomolecular systems, we discuss some practical aspects of molecular dynamics simulation techniques at constant pressure and temperature. We compare the extended Lagrangian (EL) method, initially developed by Andersen[1] for sampling from well-defined statistical mechanical ensembles, with the method by Berendsen et al.,[2] where temperature and/or pressure are kept constant by weakly coupling (WC) the system to external thermal and pressure baths. We examine the convergence of the volume and of its fluctuations (related to the system compressibility) in both approaches and compute the statistical efficiency of the two methods. Also, the influence on computed observables and fluctuations of the adjustable parameters entering the equation of motions in both approaches is discussed. Systems of increasing complexity from liquid argon to a solvated protein are examined. Remarkably, we find that observables such as volume and enthalpy obtained by extended Lagrangian and weak coupling simulations at the same thermodynamic point are within statistical error of each other. However, for values of the pressure and temperature coupling parameters used commonly in simulation of biomolecules, the statistical inefficiency of the WC approach is higher than for the EL method. This was confirmed in the study of the solvated protein. We find also that at equal computational expense the compressibility is calculated from fluctuation formulas and finite differences with similar precisions. Finally, we observe that when the solvated protein undergoes a sudden pressure increase, the volume relaxes involving two time scales: a slower one with a half-time close to 20 ps due probably to the protein internal relaxation and a faster one with a half-time of about 300 fs attributed to the solvent water. Thus, the equilibration to a new pressure of a solvated protein is 2 orders of magnitude slower than for water but occurs on a time scale manageable by current molecular dynamics simulation techniques.

I. Introduction

The study of pressure-dependent properties of systems relevant to biology such as proteins and membranes has been growing in importance in recent times.[3−5] The pressure denaturation of monomeric proteins and the dissociation of oligomers have provided many insights on the microscopic mechanism of protein folding and on the role of solvent in this process.[6−9] In addition, pressure and temperature studies of biological membranes make possible the observation of new pressure-induced phases and changes in the dynamics of the lipid of which the membranes are composed. It is clear that the exploration of phase diagrams of biological systems, even outside the biologically relevant region, can give important help in understanding the functionality of these systems.[5] Molecular modeling and simulation can be useful tools in the exploration of microscopic details corresponding to observed macroscopic behavior at high pressure and could help in the understanding of the phase diagram of these complex molecular systems. In particular, simulation could be used to calculate volume fluctuations in system such as proteins in solution or in the crystalline phase. These fluctuations have been estimated by various empirical means, but their understanding, related in a way to protein folding, is still to be clarified.[10]

In this paper we tackle the problem of how to simulate efficiently systems of increasing complexity at constant pressure. Our main motivation is to verify the feasibility of constant pressure simulation of solvated proteins. Thus, we are primarily interested in the problem of determining the volume averages and the compressibility of a molecular system. We examine and compare two different approaches to molecular dynamics (MD) simulation at constant pressure. While the extended Lagrangian (EL) method first developed by Andersen[1] is extensively used in simulation of molecular liquid, in simulation of biologically relevant systems the method invented by Berendsen and co-workers[2] of the weak coupling (WC) to an external bath is mostly used.

Andersen was the first to modify the Newtonian equations of motion to sample ensembles other than the microcanonical. In his approach the volume is a dynamical variable while the generalized force acting on this variable is proportional to the difference between the internal and an externally fixed pressure. It can be proven that the solution of the new set of equations of motion samples the isobaric−isoenthalpic (NPH) ensemble. Subsequently Parrinello and Rahman[11] showed that it is possible to write new equations of motion to simulate nonisotropic volume changes. Andersen's scheme was modified to allow for changes in the shape of the MD cell by introducing a new set of dynamical variables related to the cell metric. Thus, the fundamental idea of both methods was to represent the effect of a suitable external reservoir by adding new degrees of freedom to the system and solving the equation of motion for the new extended Lagrangian (extended Lagrangian methods). In more recent times, extended Lagrangian methods have also

* To whom correspondence should be addressed.
[⊗] Abstract published in *Advance ACS Abstracts,* February 15, 1996.

0022-3654/96/20100-4314$12.00/0

been used in combination with multiple time step r-RESPA (reversible reference system propagation algorithm) integration algorithms.[12,13]

A different approach to implement thermodynamic constraints is the *weak coupling to an external bath* of Berendsen et al.[2] They modified the Langevin equation of motion, eliminating the stochastic force and replacing the constant friction term with a variable friction proportional to the constraint. The method has been used to control temperature and pressure in simulated systems. So far there is no proof that such equations sample a statistical mechanical ensemble. Nevertheless, the simplicity of these equations and their easy implementation for complex systems have made this method popular among people modeling biomolecules.[14−18]

In this paper we study the efficiency and performance of the extended Lagrangian method and of the weak coupling method to simulate systems of increasing complexity by MD at constant pressure and temperature. We have carried out extensive simulations by both EL and WC methods of liquid argon, liquid water, and a protein, superoxide dismutase (SOD), in solution. We have paid particular attention to the choice of the external coupling parameters in both methods in order to obtain the best efficiency. We have computed the compressibility of our systems using both finite differences and fluctuation formulas (when appropriate). Anticipating our results, we find that, remarkably, the WC method gives observable averages equivalent within statistical error to those obtained at the same condition of temperature and/or pressure by EL methods. Also, we find that at equal computational expense the compressibility is calculated from fluctuation formulas and finite differences with similar precision. Finally, we observe two time scales in the volume relaxation which occurs when the solvated protein undergoes a sudden pressure increase: A slower one due probably to the protein internal relaxation, and a faster one due to the solvating water.

The paper is organized as follows: In section II we describe the methods. In section III we discuss averages and fluctuations and how thermodynamic derivatives can be computed through fluctuations. Results are discussed in section IV. The paper ends with concluding remarks.

II. Simulation Methods

A. Extended Lagrangian Method. Following the EL method, the equations of motion to simulate the isobaric−isothermal (NPT) ensemble can be derived from the Lagrangian or Hamiltonian formalism adopting a set of *virtual coordinates* related to the real set of coordinates by a noncanonical transformation. The particular form of the Lagrangian or Hamiltonian is chosen in a way that the trajectory of the system in the *extended* phase space generates the desired equilibrium distribution function upon integration over the extra (extended) variables. From the simulation point of view, an important feature of this approach is that the Hamiltonian of the extended system is a constant of motion and is, therefore, a conserved quantity during a simulation. This characteristic can be used to control the quality of the simulation.

While a detailed derivation of the EL method to simulate the NPT ensemble can be easily found in literature,[19−22] here we present only the resulting equations of motion for a system composed of interacting molecules. Such equations were those used in this study.

When dealing with molecules, one has the choice of coupling the barostat to each atomic degree of freedom or to each molecular center of mass.[19] In the former case the effect of the barostat corresponds to a space scaling that affects the position of each atom. In the latter the scaling occurs only for the position of the molecular centers of mass, thus affecting only intermolecular distances.

It is clear that the definition of the pressure tensor will depend on the chosen coupling scheme. Thus, according to the virial theorem one can write the atomic pressure for a system of N molecules:

$$P_{\mathrm{atm}} = \langle \Pi_{\mathrm{atm}} \rangle = \left\langle \frac{1}{3V} \sum_{\alpha}^{N} \sum_{i}^{N\alpha} \left(\frac{\mathbf{p}_{\alpha i}^{\,2}}{m_{\alpha i}} + \mathbf{r}_{\alpha i} \cdot \mathbf{f}_{\alpha i} \right) \right\rangle \tag{1}$$

and the molecular pressure:

$$P_{\mathrm{mol}} = \langle \Pi_{\mathrm{mol}} \rangle = \left\langle \frac{1}{3V} \sum_{\alpha}^{N} \left(\frac{\mathbf{P}_{\alpha}^{\,2}}{M_{\alpha}} + \mathbf{R}_{\alpha} \cdot \mathbf{F}_{\alpha} \right) \right\rangle \tag{2}$$

Here upper and lower case letters are used respectively for molecular and atomic properties. r is the coordinate, f the force, and V the volume. Indexes α and i apply to molecules and atoms, respectively, and N_α is the number of atoms of the αth molecule. The symbol $\langle ... \rangle$ indicates an ensemble average.

If the system is ergodic and the molecules do not dissociate (which is true for nondissociative potentials), the above pressure equations have been demonstrated to be equivalent for flexible molecules.[23] In this fashion, the choice of how to couple the barostat will not affect the results of the constant-pressure simulation but only how efficiently the system relaxes and equilibrates at a certain pressure. For rigid or for small flexible molecules coupling to the center of mass has been preferred. In the more infrequent cases of constant pressure simulation of larger flexible molecules, only atomic coupling has been employed. In this study we have chosen instead to couple the barostat to the molecular center of mass even when simulating a protein in solution. In section III we will provide arguments to justify this choice.

For ease of numerical implementation, we write all the equations of motion at constant T and P in terms of scaled coordinates. If $\mathbf{h}$ is a 3×3 matrix whose lines are the three vectors spanning the MD cell of volume $V = \det[\mathbf{h}]$, the scaled coordinates $\mathbf{s}_{\alpha i}$ of the ith atoms belonging to the αth molecule are defined according to

$$\mathbf{s}_{\alpha i} = \mathbf{h}^{-1} \mathbf{r}_{\alpha i} \tag{3}$$

where $\mathbf{r}_{\alpha i}$ are the Cartesian coordinates of the same atom. In the extended Lagrangian formulation each element of the matrix $\mathbf{h}$ is treated as an extra degree of freedom of the system. Thus, the equations of motion for the extended molecular system at external temperature T_{ext} and pressure P_{ext} are

$$\begin{aligned} m_{\alpha i} \ddot{\mathbf{s}}_{\alpha i} = {} & \mathbf{h}^{-1} \mathbf{F}_{\alpha i} - m_{\alpha i} (\mathbf{h}^{-1} (\mathbf{h}^{t})^{-1} \dot{\mathbf{h}}^{t} \dot{\mathbf{h}} + \mathbf{h}^{-1} \dot{\mathbf{h}}) \dot{\mathbf{S}}_{\alpha} + \\ & m_{\alpha i} [(\dot{\mathbf{h}}^{-1} + 2 \dot{\mathbf{h}}^{-1} \dot{\mathbf{h}} \mathbf{h}^{-1}) \mathbf{h} (\mathbf{s}_{\alpha i} - \mathbf{S}_{\alpha}) + 2 \dot{\mathbf{h}}^{-1} \mathbf{h} (\dot{\mathbf{s}}_{\alpha i} - \dot{\mathbf{S}}_{\alpha})] + \\ & m_{\alpha i} \zeta [\dot{\mathbf{h}}^{-1} \mathbf{h} (\mathbf{s}_{\alpha i} - \mathbf{S}_{\alpha}) - \dot{\mathbf{s}}_{\alpha i}] \end{aligned} \tag{4}$$

$$Q \ddot{\mathbf{h}} = (\mathbf{\Pi}_{\mathrm{mol}} - P_{\mathrm{ext}} \mathbf{1}) V (\mathbf{h}^{-1})^{t} - Q \zeta \dot{\mathbf{h}} \tag{5}$$

$$W \dot{\zeta} = \sum_{\alpha=1}^{N} \sum_{i=1}^{N_\alpha} m_{\alpha i} (\mathbf{h} \dot{\mathbf{s}}_{\alpha i})^2 + Q \, \mathrm{Tr}[\dot{\mathbf{h}}^{t} \dot{\mathbf{h}}] - g k_{\mathrm{B}} T_{\mathrm{ext}} \tag{6}$$

Here $\mathbf{S}_\alpha$ is the center-of-mass position of molecule α in scaled coordinates, $m_{\alpha i}$ is the atomic mass, and g is a constant equal to the total number of degrees of freedom of the extended system. Also, Q and W are the masses of the extended variables

h and ζ associated with the control of pressure and temperature, respectively. While P_{ext} is the applied external pressure, the molecular pressure tensor is defined by

$$\mathbf{\Pi}_{mol} = \frac{1}{V}\left[\sum_{\alpha=1}^{N} M_\alpha(\mathbf{h}\dot{\mathbf{S}}_\alpha)(\mathbf{h}\dot{\mathbf{S}}_\alpha)^t + \sum_{\alpha=1}^{N} \mathbf{F}_\alpha(\mathbf{h}\mathbf{S}_\alpha)^t\right] \quad (7)$$

where V is the volume of the simulation cell, M_α is the mass of the αth molecule, and $\mathbf{F}_\alpha = \sum_i^{N_\alpha}\mathbf{F}_{\alpha i}$ is the force acting on the center of mass of molecule α. The total internal pressure, P, can be obtained by taking the trace of eq 7, i.e.

$$P_{mol} = \langle \Pi_{mol}\rangle = {}^1/_3\langle \mathrm{Tr}\, \mathbf{\Pi}_{mol}\rangle \quad (8)$$

The first term on the right-hand side of eq 4 is the usual Newton equation of motion. The additional contributions in the second and third terms are due to the coupling with the barostat. The equations of motion for the MD cell vectors, given in eq 5, contain a force term proportional to the difference between instantaneous and the externally imposed pressure. In both eqs 4 and 5 the presence of a friction term proportional to ζ controls the total kinetic energy of the system. Finally, eq 6 is a first-order equation for the variable ζ.

We integrated the equations of motion using a Verlet based algorithm[24] modified to treat velocity dependent forces.[25] With respect to standard Verlet an iterative procedure is added to calculate the velocities of the extended system at the same time step and with similar precision as the coordinates. In our implementation, we assumed convergence when the maximum relative change between the forces on the particles and on the extended variables of two successive iterations was less than 10^{-6}.

The existence of a constant of motion is essential to verify the precision and the stability of the integration algorithm and is the only check of the correct choice of the integration time step. The iterative procedure used in the integration breaks the time reversibility of the algorithm. As a consequence, in runs longer than 1 ns, a very small energy drift is sometimes detectable.

We stress that at each time step the SHAKE[26] procedure must be repeated for each iteration to satisfy the internal constraints. Even if the convergence of the iterative algorithm is quite rapid (four or five iterations for the systems studied), for the solvated protein the CPU time used by the integrator is between 10 and 30% of the CPU time taken by the force calculation depending on the magnitude of the time step.

B. Weak Coupling Method. The approach of Berendsen et al.[2] to simulation at constant temperature is based on the idea of modifying the Langevin equations of motion in order to make the particle trajectories continuous, while maintaining the original time dependence of the temperature of the system. Thus, the particles of the system evolve without being subjected to random noise, with minimal disturbance from the Newtonian trajectory, and remaining globally coupled to the heat bath. The equation of motion now contains a time-dependent friction term which determines the strength of bath−system coupling. With similar arguments the method has been extended to constant pressure simulations.

The equations of motion of the weak coupling method, like Langevin equations, cannot be derived from a modified Hamiltonian. In terms of scaled frame coordinates for a molecular system we write

$$m_i\ddot{\mathbf{s}}_{\alpha i} = \mathbf{h}^{-1}\mathbf{F}_{\alpha i} - m_{\alpha i}A\dot{\mathbf{s}}_{\alpha i}$$
$$\dot{\mathbf{h}} = \mathbf{B}\mathbf{h} \quad (9)$$

where

$$A = \frac{1}{2\tau_T}\left(\frac{T - T_{ext}}{T}\right); \qquad \mathbf{B} = \frac{\chi_T}{3\tau_P}(\mathbf{\Pi} - P_{ext}\mathbf{1})$$

and τ_T and τ_P are coupling parameters with the dimensions of time, and χ_T is the isothermal compressibility. When τ_T and τ_P tend to infinity, these equations tend to the original microcanonical equations.

In this study we integrated the equations of motion following exactly the recipe given in the original paper. The algorithm proposed in ref 2 is a modified leapfrog in which the extra terms representing the thermostat and the barostat are included only as a first-order correction to the original Newtonian trajectory. The terms proportional to A and B introduce, to the first order, a scaling of the velocities and of the positions at each time step.

Although the solution of the equations of motion in eqs 9 is a continuous trajectory, they are not reversible in time and the total energy of the system is not a constant of motion. Nonetheless, we notice that when τ_P is infinity (i.e., constant-temperature case) and the initial total linear momentum is set to zero, the latter is conserved by the WC equations.

To present, there has not been a proof that the phase space sampled by eqs 9 correspond to any known ensemble. This is the major limitation of the WC method. In principle, the averages and the fluctuations of the thermodynamic variables calculated by the numerical solution of eqs 9 are not those of the NPT ensemble. Nevertheless, we will show later in this paper that at least averages of observables correspond to those calculated in NPT ensemble simulations.

III. Simulations and Observables

A. Implementation. We have implemented both the EL and WC methods in our in-house molecular dynamics program ORAC[27] which was originally written to carry out simulations in the microcanonical ensemble. Our program works internally in scaled coordinates, simulations are carried out using periodic boundary conditions. While the minimum image convention is implemented by the generic Fortran function ANINT or faster alternatives,[24] molecules are not reflected at the boundaries. In this way, if a protein is composed of a few non-convalently-bound subunits, these maintain their initial relative arrangement.

When simulating small molecules the cutoff of the interaction is most often applied between the molecular center of mass. This is impractical when dealing with large macromolecules. We use instead a cutoff between atomic groups. Such groups are defined to have a total charge of approximately zero. For small solvent molecules (e.g., water) the atomic group is the molecule itself, while for proteins the group depends on the electrostatic force field. Group Coulombic interactions are therefore approximately (exactly in the case of the water−water interaction) of the dipole−dipole type. During the simulation, to avoid energy conservation problems due to the handling of the electrostatic interactions, we use a cubic switching function between the groups[28] or the Ewald summation. Although, the latter technique is certainly more appropriate for systems such as proteins which contains polar and charged groups, it is computationally heavy for large samples, especially on a workstation. Thus, in this study we have preferred the use of a switched cutoff between the atomic groups.

B. Coupling the Barostat. As stated previously in this paper, the simulation results should not depend on the choice of coupling the barostat to the atoms or to the molecular centers of mass. Bearing in mind that our future applications are essentially targeted to the study of solvated proteins with internal

constraints, we have chosen the latter possibility. Our preference was based on the following considerations:

(i) It is well established for EL methods that the characteristic frequency of the extended variables (volume or metric tensor) is inversely proportional to the compressibility of the simulated ensemble. Since, experimentally, the internal compressibility of a protein is 1 order of magnitude smaller than that of water, coupling the barostat to the atoms would produce oscillations of the extended variables with at least two different time scales, slower for the water and faster for the protein. This would be likely to make the system relax slowly to equilibrium.

(ii) Related to the previous point, we observe that coupling the barostat to the atoms implies scaling the intramolecular distances, including interactions between 1−4, 1−3, and 1−2 contacts. In simulation with rigid constraints it is likely that this would have placed more computational weight on the SHAKE routine.

As will be shown later, the simulation of SOD in water confirmed a rapid relaxation of the protein volume which for a change in pressure from 0.1 to 1000 MPa occurs within 30−40 ps.

Using this choice of coupling in our simulation, we computed only the internal molecular stress tensor given in eq 2. This tensor can be divided into an ideal gas and an excess contribution. The latter can be calculated using the molecular virial as

$$\mathbf{\Pi}^{\mathrm{ex}} = \sum_{\alpha<\beta} \mathbf{r}_{\alpha\beta} \sum_{i\in\alpha} \sum_{j\in\beta} \mathbf{f}_{\alpha i\beta j} \tag{10}$$

where $\mathbf{f}_{\alpha i\beta j}$ is the mutual force between atom αi and βj. Although the coupling to the molecular center of mass avoids the calculation of the contribution to the stress tensor from eventual *intramolecular* constraints, some care must be taken in the evaluation of the molecular virial in eq 10 if a group cutoff scheme is used. If μ and ν are labeling the atomic groups, we stress that eq 10 must be computed as

$$\mathbf{\Pi}^{\mathrm{ex}} = (1/3V) \sum_{\alpha<\beta} \sum_{\mu i\in\alpha} \sum_{\nu j\in\beta} \mathbf{r}_{\alpha\beta}^{(\mu\nu)} \mathbf{f}_{\alpha\mu i,\beta\nu j} \tag{11}$$

Here $\mathbf{r}_{\alpha\beta}^{(\mu\nu)}$ is the distance between the center of mass of the images of molecules α and β corresponding to the interacting groups μ and ν.

C. Molecular Dynamics Simulations. Our simulations were carried out on systems of increasing complexity. Tests were carried out on liquid argon, liquid water, and SOD in aqueous solution. The simulation box used for liquids was chosen sufficiently large to minimize finite size effects. We simulated 256 argon atoms in a cubic cell interacting through a Lennard-Jones potential cut at 7.5 Å by a third-order cubic spline going to zero at 8 Å. The integration step varied from 1 fs (in the case of high-frequency coupling with the baths) to 6 fs. Water was simulated in a periodic box containing 250 molecules modeled with the simple point charge (SPC) model of Berendsen et al.[29] Simulations were carried out with a time step of 2 fs and using a spherical cutoff with a third order spline between 8.5 and 9 Å. We have also carried out a simulation of SPC water with Ewald summation at constant pressure and temperature to test effects on compressibility due to long-range effects.

Finally, we simulated a dimer of SOD composed of 151 amino acid residues and two metal ions, Cu and Zn, surrounded by 1457 SPC water molecules and 4 sodium counterions in an orthorhombic box. The CHARMM[28] force field was used for the protein atoms and the counterions. For the active site, a bridged metal−ligand structure formed by residues 44, 46, 61, 69, 78, 81, and 118 covalently bound to Cu and Zn, the ab initio based electrostatic model of Shen et al.[30] was used. We adopted the same cutoff and integration time step used in the simulations of pure water. All the covalent bonds were kept rigid in the MD simulation using the SHAKE algorithm. The two crystal waters close to the catalytic metals were considered as independent solvent molecules and were not bound to the copper ions.

The starting solvated SOD configuration for the constant-pressure simulations described in this study was obtained as follows: Initially, a protein molecule in its X-ray configuration[31] was placed in an orthogonal simulation box of dimensions 63 × 43 × 35 Å^3. The major inertial axis of the protein was oriented parallel to the largest dimension of the cell. Subsequently, a lattice of randomly oriented SPC waters at the standard water density at 25 °C was generated and overlapped with the original box. All the water molecules of the lattice within less than 90% of the van der Waals radius from any of the atoms of the proteins or of the two crystallization waters were eliminated. In this fashion, a new simulation box containing a SOD molecule and 1461 water molecules was obtained. To ensure electroneutrality, four of the extra waters were chosen at random and replaced by the same number of sodium ions.

To equilibrate this system, after an initial steepest-descent minimization of the potential energy, we carried out a long MD run at constant volume for 400 ps. During this period, atomic velocities were rescaled if the temperature oscillated outside a window of 20 K centered at 300 K. The final coordinates of the constant volume equilibration were used for the subsequent NPT runs discussed in this paper.

Although our program can simulate a fully flexible box, in all the calculations presented here we allow only for uniform dilation of the simulation cell. Following ref 32 this is done by imposing the constraint

$$\mathbf{h}_{\alpha\beta} = \mathbf{g}_{\alpha\beta} L \tag{12}$$

where $\mathbf{g}_{\alpha\beta}$ is a constant matrix which determines the shape of the cell and L is the extended system variable. The equations of motion can be obtained by substituting eq 12 into eqs 4−6. We implemented uniform dilation only for orthogonal boxes.

D. Simulation Efficiency and Thermodynamic Derivatives. The efficiency of a simulation was monitored by computing the so-called statistical inefficiency s_A for some observable A. This quantity corresponds to twice the observable decorrelation time, τ_A, defined as the time lag between points of a trajectory for which a given observable A can be considered uncorrelated. τ_A was estimated from simulation according to[24]

$$\tau_A = \int_0^\infty \mathrm{d}t\, C_{AA}(t)/C_{AA}(0) \tag{13}$$

where $C_{AA}(t)$ is the time-dependent autocorrelation function of the fluctuation of A (δA), i.e.

$$C_{AA}(t) = \langle \delta A(t)\, \delta A(0) \rangle \tag{14}$$

With the knowledge of τ statistical errors on observables and fluctuations were computed following well-known procedures.[33,24]

We have also tested the performance of the EL and WC method against the calculation of thermodynamic derivatives, such as bulk modulus and specific heat. These derivatives were computed from the fluctuations of the corresponding observables and from finite differences of the observables at two state points.

In the *NPH*, *NPT*, and canonical (*NVT*) ensembles we have used the following well-known formulas:

Isothermal compressibility (or inverse isothermal bulk modulus):

$$\chi_T = B_T^{-1} \equiv -\frac{1}{V}\left(\frac{\partial V}{\partial P}\right)_{NT} = \beta\frac{\langle \delta V^2\rangle_{NPT}}{\langle V\rangle_{NPT}} \tag{15}$$

Adiabatic compressibility (or inverse adiabatic bulk modulus):

$$\chi s = B_s^{-1} \equiv -\frac{1}{V}\left(\frac{\partial V}{\partial P}\right)_{NS} = \beta\frac{\langle \delta V^2\rangle_{NPH}}{\langle V\rangle_{NPH}} \tag{16}$$

Constant-volume specific heat:

$$c_v \equiv \left(\frac{\partial E}{\partial T}\right)_{NV} = \frac{1}{k_B T^2}\langle \delta E^2\rangle_{NVT} \tag{17}$$

Constant-pressure specific heat:

$$c_P \equiv \left(\frac{\partial H}{\partial T}\right)_{NP} = \frac{1}{k_B T^2}\langle \delta H^2\rangle_{NPT} \tag{18}$$

Specific heat and compressibility were also computed by finite difference by taking the slope between adjacent points of the functions $-\ln(V(P))$ and $H(T)$, respectively. The maximum error was then estimated as half the difference between the minimum and maximum slope.

IV. Results

A. Extended Variables and Coupling Parameters. In the EL method the detailed dynamics of the extended variables depends upon the value of the corresponding masses chosen. Within certain approximations the associated fundamental frequencies can be readily estimated by linearizing the equations of motion in **h** and ζ (eqs 5 and 6, respectively). Thus, in the limit of large Q, the barostat mass, and small W, the thermostat mass, it can be shown[32] that the characteristic oscillatory frequencies for the variables **h** and ζ are given by

$$\omega_Q = (3LB/Q)^{1/2} \tag{19}$$

while ζ behaves as an harmonic oscillator with frequency

$$\omega_W = (2Nk_BT/W)^{1/2} \tag{20}$$

When the time scales of **h** and ζ are similar, eqs 5 and 6 couple together and their characteristic frequencies can differ significantly from their harmonic values. The best choice of the pressure and temperature mass parameters would provide a direct coupling to those vibrational modes of the system directly involved in the processes of sound and thermal diffusion, respectively. Since low-frequency modes ($\nu < 100$ cm^{-1}) bring the highest weight in both phenomena, one is obliged to choose a barostat and thermostat masses with the same order of magnitude. Thus, the harmonic frequencies given by eqs 19 and 20 can be used only as rough estimates of the real time scales. As an example, if we choose Q and W corresponding to an ω_Q and ω_W of 50 and 150 cm^{-1}, respectively, the *experimental* ω_Q was found at 130 cm^{-1}. To determine the mass Q from eq 19 we used a bulk modulus of 132 MPa for the simulation of liquid argon and of 1890 MPa for liquid water and SOD in solution.

In contrast with the oscillatory behavior of the extended variables discussed above, due to the second-order character of the EL equations, the volume and temperature in WC simulations do not show such periodic behavior. From a simulation at $P = 0.1$ MPa and $T = 100$ K of liquid argon, we present in Figure 1 the volume fluctuation time autocorrelation function in frequency space for some value of the pressure coupling parameter, τ_P, and compare it with results from NPH simulations.

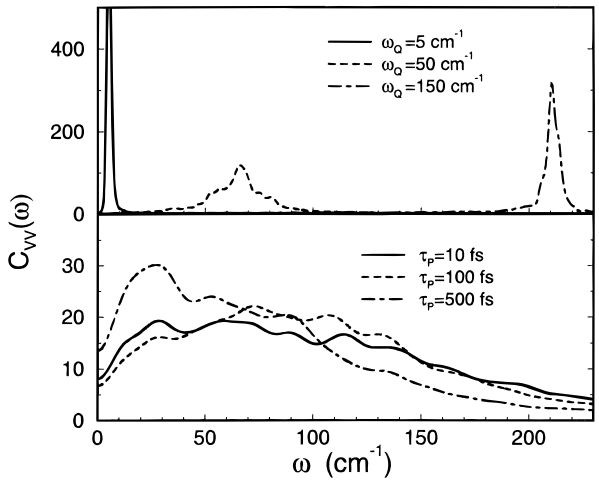

Figure 1. Spectrum of volume fluctuations for argon at $P = 0.1$ MPa and $T = 100$ K obtained with the EL (top) and the WC method (bottom) for different values of the *barostat mass* ω_Q and of the coupling constant τ_P, respectively. The spectrum of volume fluctuations is defined as $C_{VV}(\omega) = \int_0^\infty dt\, C_{VV}(t)\cos(\omega t)$ where $C_{VV}(t) = \langle \delta V(t)\delta V(0)\rangle/\langle(\delta V(0))^2\rangle$ is the normalized time autocorrelation function of the cell volume fluctuations. Frequencies ω and ω_Q are expressed in cm^{-1}.

It is clear from this figure that in the WC simulations there are no specific-volume fluctuation modes which could be used as a viable criterion for the choice of τ_P. In the following section we examine the effect of various choices of τ_P and τ_T on the observables of the simulated system.

B. Averages and Fluctuations. In Tables 1 and 2 we present observable averages and fluctuations of a simulation of 256 argon atoms. Runs were carried with the WC and the EL methods using various coupling parameters, τ_P and τ_T, and extended variable masses, ω_Q and ω_W, respectively.

Table 1 shows that the thermostating efficiency of the WC equations decreases strongly with the increase of τ_T. In particular, at high τ_T the temperature is not kept at the chosen value. As a consequence, the observed changes in average volume (V in column 11) computed with different coupling parameters are due mainly to changes in temperature. We verified that the changes in volume between runs at the same pressure but at a slightly different temperature were in agreement with the coefficient of thermal expansion.

We also notice that temperature and pressure fluctuations (δT and δP in columns 5 and 7, respectively) tend to zero as τ_P and τ_T become smaller in the strong coupling limit. In the opposite conditions, when τ_P and τ_T are large, these fluctuations tend to those of the microcanonical ensemble, while enthalpy and volume fluctuations (δH and δV in columns 10 and 12, respectively) go to zero, i.e., their microcanonical value. Conversely, in the strong coupling limit these fluctuations reach values similar, but not identical, to those of the NPT ensemble. Since fluctuations in the WC method depend on the coupling parameters both in the strong and weak coupling regimes, the generated ensemble is not only unknown but also changes with changes in the τ_P and τ_T parameters.

As shown in Table 2, the temperature control obtained by the EL runs is more effective than in WC simulations. In addition, the observables and their fluctuations show no

TABLE 1: Weak Coupling Method: Liquid Argon[a]

τ_P	τ_T	T	T	δT	P	δP	U	H	δH	V	δV	c_P	B	s_V
18	18	0.3	100.0	0.7	0.1	0.2	−4.758	−3.51	0.10	13686	250	3.81	303	1.4
30	30	0.6	100.0	1.0	0.1	0.3	−4.754	−3.50	0.11	13706	268	4.38	266	2.4
150	150	1.2	100.0	2.3	0.1	1.4	−4.761	−3.51	0.09	13684	223	2.68	384	3.0
300	300	0.6	99.9	2.6	0.1	2.4	−4.763	−3.51	0.07	13685	196	1.84	482	
750	750	0.6	99.6	2.9	0.1	4.0	−4.774	−3.53	0.05	13654	169	1.11	669	
1500	1500	0.6	99.4	3.0	0.1	5.1	−4.787	−3.54	0.04	13622	131	0.65	1063	6.0
4500	4500	0.6	99.1	3.0	0.1	6.4	−4.788	−3.55	0.03	13618	86	0.24	2575	12.0
6000	6000	2.4	99.0	3.3	0.1	7.7	−4.796	−3.56	0.02	13596	83	0.20	2654	
10000	10000	2.0	98.4	3.0	0.1	7.0	−4.817	−3.59	0.01	13547	57	0.08	6024	13.0

[a] Simulation parameters, averages, and corresponding fluctuations for a system of 256 argon atoms. WC coupling parameters τ_P and τ_T are given in fs, the length of the trajectory T in ns, average temperature T in K, average pressure P and isothermal bulk modulus B_T in MPa, average potential energy U and enthalpy H in kJ/mol, average volume V in Å^3, constant pressure specific heat c_P in units of k_B per molecule, and statistical inefficiency s in ps.

TABLE 2: Extended Lagrangian Method: Liquid Argon[a]

ω_Q	ω_W	T	T	δT	P	δP	U	H	δH	V	δV	c_P	B	s_V
100	50	0.6	100.0	5.1	0.1	10.1	−4.764	−3.51	0.13	13684	302	6.28	207	1.9
60	150	0.6	100.0	5.1	0.1	9.4	−4.747	−3.50	0.13	13727	299	6.05	212	
20	50	0.6	100.0	5.0	0.2	10.4	−4.759	−3.51	0.13	13690	296	6.02	216	1.5
10	25	0.6	100.0	5.1	0.2	10.5	−4.760	−3.51	0.13	13690	295	6.13	217	1.4
4	10	0.6	100.0	5.0	0.2	10.7	−4.756	−3.51	0.14	13704	316	6.99	190	
1	2	2.0	100.0	4.4	0.1	9.4	−4.754	−3.50	0.12	13705	284	5.59	234	

[a] Simulation parameters, averages, and corresponding fluctuations for a system of 256 argon atoms. EL masses ω_Q and ω_W are given in cm^{-1}. Other symbols and units as in Table 1.

TABLE 3: Weak Coupling Method: Liquid Water[a]

T	T_{ext}	P_{ext}	H	V	c_P^{FD}	B_T^{FD}
0.3[b]	275	0.1	−37.094 ± 0.015	7529.0 ± 6.9	10.19 ± 0.74	
0.9[a]	300	0.1	−34.964 ± 0.009	7638.4 ± 4.2	10.31 ± 0.39	1710 ± 300
0.3[b]	325	0.1	−32.809 ± 0.021	7795.1 ± 8.7	10.43 ± 0.82	
0.3[b]	300	250	−31.442 ± 0.015	6930.3 ± 5.4		3330 ± 200
0.3[a]	300	500	−28.096 ± 0.015	6528.9 ± 4.4		4800 ± 330
0.3[a]	300	750	−24.849 ± 0.014	6234.1 ± 3.4		6020 ± 680

[a] Simulation parameters and average thermodynamic properties for a system of 250 SPC water molecules. WC couplings are $\tau_P = \tau_T = 300$ (*a*) or $\tau_P = \tau_T = 200$ (*b*). T_{ext} and P_{ext} are the external temperature in K and pressure in MPa, respectively; other symbols and units are the same as in Table 1. Thermodynamical derivatives are computed by finite difference (FD). B_T^{FD} (c_P^{FD}) is the slope between adjacent points of $-\ln(V(P))$ ($H(T)$). The error is half the difference between minimum and maximum slope. To obtain values of B_T^{FD} (c_P^{FD}) at the desired P (T), we used a linear interpolation and propagated the error. Errors reported is 1 standard deviation, except for FD values where the error is the maximum error. Errors have been computed assuming a decorrelation time of 1.67 ps (decorrelation time of the observable *volume* at atmospheric pressure).

dependence, within statistical error from the strength of the temperature and pressure baths. This is true for a wide range of values of the extended variable masses. A limitation in the choice of the mass is that a smaller mass requires a shorter integration time step to correctly integrate the equations of motion. On the other hand, if the mass is too large, convergence of averages and fluctuations becomes slow.

The efficiency of phase space sampling characteristic of a simulation method can be estimated through the decorrelation time for the volume, τ_V, defined in section IIID. In the last column of Tables 1 and 2 we present the corresponding statistical inefficiency, $s_V = 2\tau_V$. We point out that for other observables such as energy and enthalpy similar values were obtained. While in the EL simulation the statistical inefficiency is weakly dependent on the mass parameters, in the WC runs s_V is higher and increases markedly when the strength of the coupling with the bath decreases. From these results, it seems that the EL method is in general more efficient than the WC method. We stress however that even though the WC simulations do not sample from any known ensemble, remarkably, their observable averages agree well with those calculated by NPT ensemble simulations.

C. Thermodynamic Derivatives. In this section we examine the problem of computing efficiently thermodynamic derivative by constant-temperature and -pressure simulations. We focused our attention on liquid water. A system composed of 250 SPC water molecules was simulated at $P = 0.1$, 250, 500, and 750 MPa and $T = 275$, 300, and 325 K. Simulations by the EL method were performed with barostat and thermostat masses equivalent to ω_W and $\omega_Q = 30$ cm^{-1}. The coupling parameters for the WC runs were $\tau_P = \tau_T = 300$ fs and 200 fs as indicated in Table 3.

By comparing results in Tables 3 and 4, we find that both methods compute observables such as volume and enthalpy which are within the statistical error of each other (unless otherwise stated, by *error* we refer to the maximum error, i.e., 3 times the standard deviation σ). At the same time the decorrelation time of the WC simulation is confirmed (at least for the strength of coupling we used) to be higher than for the EL runs. We found 0.9 and 1.7 ps for the EL and WC simulations, respectively.

In Tables 3 and 4 the characteristic errors on the enthalpy and volume for a typical 300 ps simulation run are less than 0.35%. On the other hand, the relative error on fluctuations is larger on the order of 15%. On a longer trajectory of 0.9 ns, errors on the volume and its fluctuations are reduced to 0.16 and 9.3%, respectively.

Thermodynamic derivatives can also be computed numerically by carrying out simulations at two or more different thermodynamic points. In Figure 2 we compare the bulk modulus calculated with both methods at $T = 300$ K as a function of pressure using the corresponding fluctuation formula

TABLE 4: Extended Lagrangian Method: Liquid Water[a]

	T	T_{ext}	P_{ext}	H	V	c_P	c_P^{FD}	B_T	B_T^{FD}
	0.3	275	0.1	-37.154 ± 0.025	7530.3 ± 6.5	10.00 ± 0.54	10.80 ± 0.51	1970 ± 110	
	0.9	300	0.1	-34.926 ± 0.016	7642.4 ± 4.0	10.61 ± 0.33	10.56 ± 0.27	1883 ± 59	1900 ± 290
	0.3	325	0.1	-32.757 ± 0.025	7802.9 ± 7.7	10.50 ± 0.57	10.32 ± 0.56	1728 ± 93	
	0.3	300	250	-31.424 ± 0.028	6938.0 ± 4.9	9.88 ± 0.53		3510 ± 190	3320 ± 180
	0.3	300	500	-28.075 ± 0.027	6522.8 ± 4.0	9.93 ± 0.53		4890 ± 260	4810 ± 330
	0.3	300	750	-24.810 ± 0.024	6235.7 ± 3.3	7.70 ± 0.42		6700 ± 360	6310 ± 730
Ewald	0.6	300	0.1	-33.804 ± 0.018	7790.8 ± 5.1	8.59 ± 0.33		1784 ± 68	

[a] Simulation parameters and average thermodynamic properties for a system of 250 SPC water molecules. Thermodynamical derivatives are computed by mean of fluctuations and by finite difference (FD). Other symbols and units are the same as in Table 3. Errors have been computed assuming a decorrelation time of 0.87 ps.

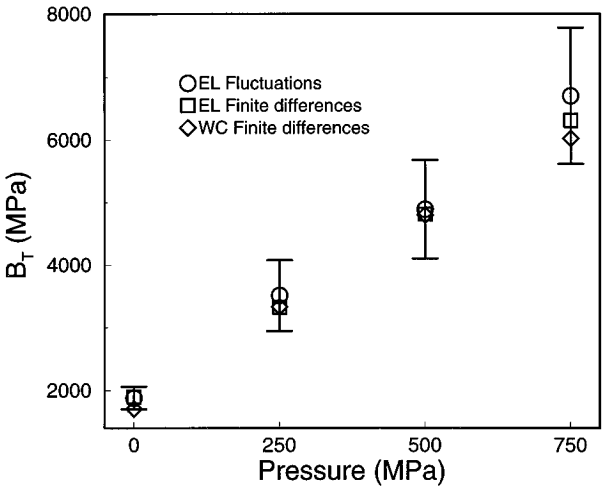

Figure 2. Isothermal bulk modulus as a function of pressure, both expressed in MPa. Circles correspond to bulk modulus obtained from volume fluctuations with the EL method, squares (EL) and diamonds (WC) correspond to the differential expression computed through finite differences. The error bar is 3 times the standard deviation and refers to the fluctuation results.

and finite differences. The results from the WC simulation could be computed only from finite differences given the strong dependence of the fluctuations on the bath coupling parameters. We notice that the bulk modulus computed via the two approaches at the same thermodynamic point coincide within statistical error. In the pictures the error bar is equal to three standard deviations σ. Also, Figure 2 shows the agreement between results obtained with WC and EL simulations.

As shown in Tables 3 and 4, the relative error of the bulk modulus calculated by numerical derivatives never exceeds 12%, in the most defavorable case, which compares with a maximum error of the fluctuations of about 17%. Considering that the bulk modulus and in general thermodynamic derivatives can be calculated by fluctuation formulas in only one MD simulation, it is clear that the improvement in efficiency obtainable by the alternative finite difference method is scarce. In addition, it must be pointed out that in calculating a numerical derivatives we neglect all the higher order contributions. As shown in Table 4, this assumption might be valid for the specific heat which does not vary very much between 275 and 325 K. On the contrary, results for the bulk modulus show a pronounced nonlinear dependence upon pressure between 0.1 and 750 MPa. This will be confirmed by the study on the protein in solution, described in the following section.

We have also performed a simulation of SPC water in the NPT ensemble using the Ewald summation method to compute the electrostatic energy and forces. We show the results in the last line of Table 4. Both the specific heat and bulk modulus are found to be within statistical uncertainty of the values calculated with the spherical cutoff. On the contrary, the differences in enthalpy and volume are higher. Using Ewald summation, the density at atmospheric pressure is calculated as 968.4 kg/m^3, lower than the experimental density of 996.6 kg/m^3 and the value of 984.8 kg/m^3 calculated with a spherical cutoff.

To quantify the effect of the long-range Coulomb forces on pressure and energy, we carried out simulations in the microcanonical ensemble with and without the Ewald sum at the density obtained at atmospheric pressure using the spherical cutoff (984.8 kg/m^3). The calculated difference in pressure is $P_{Ew} - P_{cutoff} = 39.8$ MPa, while the difference in energy is $E_{Ew} - E_{cutoff} = 1.0$ kJ/mol. Effects on the pressure due to the cutoff on the Lennard-Jones part of the potential can be estimated[24] at -32 MPa. Thus, long-range electrostatic and Lennard-Jones corrections to the pressure seem roughly to compensate.

D. Volume Relaxation in Complex Molecular Systems. To verify the feasibility of high-pressure simulation of biomolecular systems, we have investigated how the volume of a solvated protein relaxes when the external pressure is changed.

We carried out three runs of the dimeric protein SOD in solution at pressures $P = 0.1$, $P = 1000$, and $P = 2000$ MPa. The run at lower pressure was started from a configuration obtained after 400 ps of equilibration at constant volume. After 100 ps of equilibration at 0.1 MPa with the EL method in the NPT ensemble, we performed the three simulations in sequence of ascending pressure using the last configuration of each simulation as the starting configuration for the next. The temperature was fixed at 300 K, and each trajectory was 120 ps long. We will provide a full account of the results on a forthcoming paper.[34] As a test of the WC method, we also performed a separate WC run at 1000 MPa starting from the same EL equilibrated configuration at 0.1 MPa used for the EL run at 1000 MPa. The extended variable masses used in the EL runs were $\omega_Q = 15$ cm^{-1} and $\omega_W = 30$ cm^{-1}, while for the WC simulation we used $\tau_P = \tau_T = 150$ fs.

In Figure 3 we plot the simulation box volume as a function of the simulation time. Also, in Figure 4 we plot the evolution of the Voronoi volume of the entire protein for the three runs. The calculation of the Voronoi volume was carried out with the algorithm of ref 35, including in the computation only nonhydrogen atoms.

In Figure 5 we compare the evolution of the enthalpy for a EL and WC run when the pressure was changed from 0.1 to 1000 MPa. Although the equilibrium value attained by the two simulations is similar the WC run relaxes more slowly than the EL run. This confirms the higher statistical inefficiency of the former method. We stress that in this run we used a pressure coupling parameter similar to those used in other biomolecular simulations.

Nonetheless, for all the EL and WC runs the internal pressure converges very rapidly to the desired value. This finding for the simulations with the WC method contradicts Kitchen et al.[14]

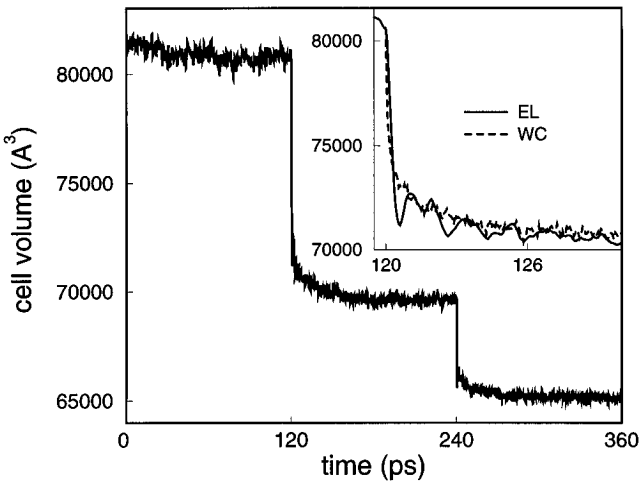

Figure 3. Relaxation of volume of the whole simulation cell composed by one SOD dimer solvated by 1457 water molecules. The system, initially at atmospheric pressure, has been brought at 1000 MPa after 120 ps of simulation, and at 2000 MPa after an additional 120 ps. In the inset, the relaxation of the volume obtained by both EL (solid line) and WC method (dashed line).

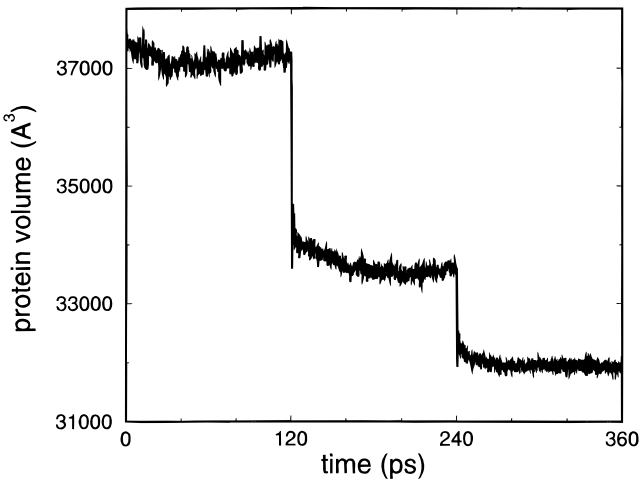

Figure 4. Relaxation of Voronoi volume of the SOD dimer at the same conditions described in Figure 3.

who reported problems in attaining the imposed pressure. The pressure of their 100 ps long simulation of BPTI in water carried out with a $\tau_P = 100$ fs converged at 10 MPa instead of 0.1 MPa.

By visual inspection of Figures 3 and 4, we notice that the volume relaxation occurs with time scales on the order of a few tens of picoseconds. To quantify this decay time, we have calculated the decay function of the volume (V) defined as

$$F(t) = \frac{V(t) - V(\infty)}{V(0) - V(\infty)} \tag{21}$$

In Figure 6, we show $F(t)$ for the total volume of the simulation box and for the protein Voronoi volume. As a reference, in the same picture we have plotted this function for pure SPC water which was obtained from a sample made out of 686 molecules of water. The system, equilibrated at 300 K and atmospheric pressure (0.1 MPa), was suddenly brought to a pressure of 1000 MPa and followed for 45 ps.

We notice that in these EL runs the periodic volume oscillations are superimposed on the decaying behavior. Although the frequency of oscillation of the cell volume depends on the choice of the barostat mass, we verified for the pure

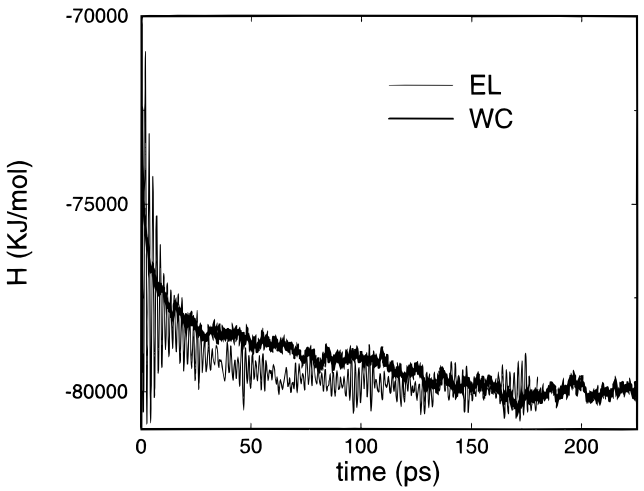

Figure 5. Enthalpy relaxation for SOD in solution as the pressure changes from 0.1 to 1000 MPa using EL (thin line) and WC (thick line) method. The initial configuration for both trajectories is the same. The EL trajectory has been continued up to 180 ps, WC trajectory up to 225 ps.

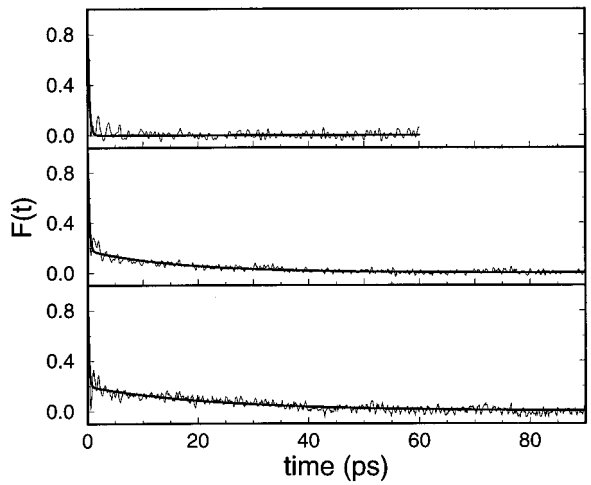

Figure 6. Decay function (thin line) $F(t)$ for the cell volume of pure water (top), of solvated SOD (middle), and for protein volume computed through the Voronoi method (bottom). The system is initially at equilibrium at atmospheric pressure. At $t = 0$ the pressure is instantaneously changed to 1000 MPa. The thick lines are least-squares fits to $F(t)$. Fit functions are $\exp(-t/\tau)$ for pure water and $A\exp(-t/\tau_{fast}) + (1 - A)\exp(-t/\tau_{slow})$ for solvated SOD cell and Voronoi volume.

water simulation that, unless this mass is very high, the relaxation time scale does not depend on its value.

Volume relaxation is fast for pure water: It takes less than a picosecond for the system to relax to its equilibrium density. We find that $F(t)$ can be modeled by a simple exponential $F(t) = Ae^{-t/\tau}$ with $\tau \sim 300$ fs. On the contrary, the relaxation of the solvated SOD protein is more complex and cannot be fitted by a single exponential. We find that a fit to a double exponential gives the best results for both the total cell volume and the protein Voronoi volume. For the total cell volume the best fit gives $\tau^T_{slow} \simeq 15$ ps and $\tau^T_{fast} \simeq 300$ fs, and $\tau^V_{slow} \simeq 20$ ps and $\tau^V_{fast} \simeq 200$ fs for the Voronoi volume. The similarity in the time scale of the fast relaxation in the protein and the decay time obtained for pure water suggests that τ_{slow} and τ_{fast} have to be related to the relaxation of the protein and of the solvating water, respectively.

We also attempted to fit the decay to a stretched exponential which typically models relaxation processes in glassy systems. However, the double exponential was found to produce the best fit.

We are aware that ours is only a rough estimate of the decay times. A series of nonequilibrium runs would have to be carried out to obtain more reliable values.

V. Concluding Remarks

In this paper we have tested efficiency and performance of alternative constant-pressure and/or temperature simulation methods against calculation of observables and of their thermodynamic derivatives. We have carried out simulations for systems of increasingly complexity using the extended Lagrangian and the weak coupling methods. The latter technique is most popular in biomolecular modeling. Remarkably, we find that observables such as volume and enthalpy obtained by EL and WC simulations at the same thermodynamic point are within statistical error of each other. The same agreement was found for the bulk modulus and specific heat computed with finite differences. However, for values of the pressure and temperature coupling parameters used commonly in simulation of biomolecules, the statistical inefficiency of the WC approach is higher than for the EL method. This was confirmed in the study of a protein in solution.

We have also calculated thermodynamic derivatives from fluctuation formulas in the NPT ensemble by the EL method and found that they agree within statistical error with results obtained from finite differences. Considering that the bulk modulus and in general thermodynamic derivatives can be calculated by fluctuation formulas in only one MD simulation, we find that the improvement in efficiency attainable by the alternative finite difference method is small.

Finally, we have investigated the relaxation of a solvated protein when the pressure is suddenly increased. The equilibration to a new pressure is 2 orders of magnitude slower than for water, but it occurs in time scale, 30−40 ps, manageable by current MD simulation techniques.

Acknowledgment. We would like to thank Piero Procacci for useful discussion and for helping us in the calculation of the Voronoi volumes.

References and Notes

(1) Andersen, H. *J. Chem. Phys*. **1980**, *72*, 2384.
(2) Berendsen, H.; Postma, J.; van Gunsteren, W.; DiNola, A.; Haak, J. *J. Chem. Phys*. **1984**, *81*, 3684.
(3) Frauenfelder, H.; Alberding, N.; Ansari, A.; Braunstein, D.; Cowen, B.; Hong, M.; Iben, I.; Johnson, J.; Luck, S.; Marden, M.; Mourant, J.; Ormos, P.; Reinisch, L.; Scholl, R.; Shulte, A.; Shyamsunder, E.; Sorensen, L.; Steinbach, P.; Xie, A.; Young, R.; Yue, K. *J. Phys. Chem*. **1990**, *94*, 1024.
(4) Silva, J.; Weber, G. *Annu. Rev. Phys. Chem*. **1993**, *44*, 89.
(5) Jonas, J.; Jonas, A. *Annu. Rev. Biophys. Biomol. Struct*. **1994**, *23*, 287.
(6) Zipp, A.; Kauzmann, W. *Biochemistry* **1973**, *12*, 4217.
(7) Li, T.; Hook, J. W.; Drickamer, H. G.; Weber, G. *Biochemistry* **1976**, *15*, 5571.
(8) Weber, G. *J. Phys. Chem*. **1993**, *97*, 7108.
(9) Peng, X. D.; Jonas, J.; Silva, J. L. *Biochemistry* **1994**, *33*, 8223.
(10) Cooper, A. *Prog. Biophys. Mol. Biol*. **1984**, *44*, 181.
(11) Parrinello, M.; Rahman, A. *J. Appl. Phys*. **1981**, *52*, 7182.
(12) Tuckerman, M. E.; Berne, B.; Martyna, G. *J. Chem. Phys*. **1992**, *97*, 1990.
(13) Procacci, P.; Berne, B. J. *Mol. Phys*. **1994**, *835*, 255.
(14) Kitchen, D.; Reed, L.; Levy, R. *Biochemistry* **1992**, *31*, 10083.
(15) Stouch, T. *Mol. Sim*. **1993**, *10*, 335.
(16) Bassolino-Klimas, D.; Alper, H. E.; Stouch, T. *Biochemistry* **1993**, *32*, 12624.
(17) Marrink, S.-J.; Berendsen, H. *J. Chem. Phys*. **1994**, *98*, 4155.
(18) Egberts, E.; Marrink, S.-J.; Berendsen, H. *Eur. Biophys. J*. **1994**, *22*, 423.
(19) Ferrario, M.; Ryckaert, J.-P. *Mol. Phys*. **1985**, *54*, 587.
(20) Nosé, S. In *Computer Simulation in Materials Science*; Meyer, M., Pontikis, V., Eds.; Kluwer Academic Publishers: Dordrecht, 1991; p 21.
(21) Nosé, S. *Prog. Theor. Phys. Supp*. **1991**, *103*, 1.
(22) Ferrario, M. In *Computer Simulation in Chemical Physics*; Allen, M. P., Tildesley, D. J., Eds.; Kluwer Academic Publishers: Dordrecht, 1993; p 153.
(23) Ciccotti, G.; Ryckaert, J.-P. *Comput. Phys. Rep*. **1986**, *4*, 345.
(24) Allen, M. P.; Tildesley, D. J. *Computer Simulation of Liquids*; Oxford University Press: Oxford OX2 6DP, 1989.
(25) Ryckaert, J.-P.; Ciccotti, G. *J. Chem. Phys*. **1983**, *78*, 7368.
(26) Ryckaert, J.-P.; Ciccotti, G.; Berendsen, H. *J. Comput. Phys*. **1977**, *23*, 327.
(27) Marchi, M. ORAC—A Molecular Dynamics Program to Simulate Complex Systems.
(28) Brooks, B. R.; Bruccoleri, R. E.; Olafson, B. D.; States, D.; Swaminanthan, S.; Karplus, M. *J. Comput. Chem*. **1983**, *4*, 187. The potential parameters and topology used in the SOD simulations were taken from the Parameter and Topology files for CHARMM version 20, Release 1989.
(29) Berendsen, H. J. C.; Postma, J. P. M.; van Gunsteren, W. F.; Hermans, J. In *Intermolecular Forces*; Pullman, B., Ed.; Reidel: Dordrecht, 1981.
(30) Shen, J.; Wong, C. F.; Subramiam, S.; Albright, T. A.; McCammon, J. A. *J. Comput. Chem*. **1990**, *11*, 346.
(31) Tainer, J. A.; Getzoff, E. D.; K. M. Beem, J. S. R.; Richardson, D. C. *J. Mol. Biol*. **1982**, *160*, 181.
(32) Nosé, S.; Klein, M. *Mol. Phys*. **1983**, *50*, 1055.
(33) Jacucci, G.; Rahman, A. *Nuovo Cimento* **1984**, *D4*, 341.
(34) Paci, E.; Marchi, M., to be submitted.
(35) Procacci, P.; Scateni, R. *Int. J. Quantum Chem*. **1992**, *42*, 1515.

JP9529679